

Hybrid Microfabricated Device for Field Measurement of Atmospheric Sulfur Dioxide

Shin-Ichi Ohira and Kei Toda*

Department of Environmental Science, Faculty of Science, Kumamoto University, 2-39-1 Kurokami, Kumamoto 860-8555, Japan

Shin-Ichiro Ikebe

Aso Volcano Museum, Kusasenri, Aso, Kumamoto 869-2200, Japan

Purnendu K. Dasgupta

Department of Chemistry and Biochemistry, Texas Tech University, Lubbock, Texas 79409-1061

A miniaturized planar-membrane-based gas collector of 800 nL internal liquid volume was integrated with a microfabricated conductivity detector to measure atmospheric SO₂. This device is operated with a dilute H₂SO₄/H₂O₂/2-propanol absorber for a finite integration period (typically, 1.5 min) without liquid flow. During this period, sulfuric acid is formed from SO₂ that diffuses into the liquid and accumulates therein. The increase in conductivity with ongoing sampling is measured. The absorber is then replaced with fresh solution, and the process starts anew. The most important factors that govern sensitivity and the detection limit are the choice of the membrane, the nature of the internal collector solution, and the thickness of the solution layer. A porous polypropylene membrane with some 2-propanol (IPA) incorporated in the internal solution was found to be the best combination. The sensitivity was inversely proportional to the solution layer thickness, and a layer thickness of 100 μm resulted in a practical device with good performance characteristics. Greater applied pressure on the gas phase relative to the liquid side also can improve device performance. The system is operated with 12 V DC and does not require a liquid pump. Under optimized conditions, the LOD is 0.7–1.0 ppbv for a sampling period of 1.5 min. The device was field-tested around Mt. Aso in Japan. Changes in ambient SO₂ concentrations could be followed with good time resolution. The results are compared with data obtained by a collocated macroscale instrument.

Sulfur dioxide (SO₂) is one of the most important inorganic air pollutants. Its emission and ambient concentration have been regulated for several decades. In Japan, recent advances in desulfurization methods and equipment have lowered SO₂ levels in urban areas significantly below the regulated value (the Japanese standard is 40 ppbv for the daily average¹); typically the daily average is one to several ppbv. However, much greater

average concentrations of SO₂ prevail in developing countries where the sulfur content of fossil fuels consumed is much higher and desulfurization equipment is nonexistent or nonfunctional. In many areas of Japan, SO₂ originating from volcanic emissions, quite aside from anthropogenic sources, represents a significant threat. In Kumamoto, Japan, within the last 5 years, spectators have died from SO₂ inhalation while watching the volcanic crater of Mt. Aso.² Sulfur dioxide damages the respiratory organs, and although the maximum permissible time weighted average in the workplace is 5 ppmv,³ asthmatic patients can have severe attacks even at a 200 ppbv concentration.⁴ Near volcanoes, fumaroles, or even in heavily industrialized areas in developing countries, prevailing meteorological conditions can cause alarmingly high concentrations of SO₂. It is also now generally agreed that forthcoming major volcanic eruptions will sensitively monitored for increasing sulfur gas emissions as indicated by increasing seismic activity. Widespread deployment of affordable, low maintenance, sufficiently sensitive SO₂ measurement sentinel instrumentation thus awaits a mass-manufacturable device that meets these qualifications.

A great many methods have been used to measure atmospheric SO₂. In the United States, the Federal Reference Method for the colorimetric measurement of SO₂ involves collection in an aqueous tetrachloromercurate(II) solution, followed by reaction with formaldehyde and *p*-rosaniline.⁵ A simpler method based on solution conductometry is well-known; this utilizes the high solubility of SO₂ (Henry's law constant is 1.2 M/atm at 25 °C⁶) and constitutes the basis of standard methods in many countries,

- (1) *Environmental quality standards in Japan*; <http://www.env.go.jp/en/lar/regulation/aq.html>.
- (2) Kinoshita, K.; Ikebe, S.; Kanegaki, C.; Naoe, H.; Imamura, K. *Shizen Saigai Kagaku Kenkyujo Seibuchiku-Bukai Ronbunshu*, **1998**, 22, 133–138.
- (3) *About sulfur dioxide*; <http://www.amgas.com/so2.htm>
- (4) *Air quality guideline, WHO 1999*; <http://www.who.int/environmental-information/Air/Guidelines/Chapter3.htm>
- (5) West, P. W.; Gaeke, G. C. *Anal. Chem.* **1956**, 12, 1816–1819.
- (6) (a) <http://www.mpch-mainz.mpg.de/~sander/res/henry.html>. (b) Maahs, H. G.; In *Heterogeneous Atmospheric Chemistry*; Schryer, D. R. Ed.; Geophysical Monograph 26; American Geophysical Union: Washington D. C., 1982; pp 187–195.

* E-mail: todakei@sci.kumamoto-u.ac.jp.

including Japan.⁷ Sulfur dioxide concentration can be measured from the conductivity increase corresponding to the amount of sulfurous acid formed from the dissolution of SO_2 .^{8,9} When an oxidant is added into the absorbing solution, it is further oxidized to H_2SO_4 . Each molecule of H_2SO_4 releases two protons, whereas under the operating conditions, sulfurous acid behaves as a monoprotic acid. Further, the oxidative process aids additional dissolution of SO_2 . Thus, the sensitivity becomes significantly higher with the addition of an oxidant, such as hydrogen peroxide.^{10–12} Thus solution conductometry has been adopted as a Japanese industrial standard method⁷ and is widely used. However, the sampled gas is bubbled through a large volume of the absorbing solution in this method, and thus, long accumulation times (e.g., 60 min) are needed in order to obtain enough concentration of analyte in the solution to measure urban background levels of SO_2 .

For the collection of gaseous SO_2 , a variety of devices, including denuders, tubular diffusion scrubbers, liquid drops,¹⁰ and films,¹¹ etc., have been investigated. With denuders, coatings of PbO_2 ,^{12,13} Cu/CuO ,¹⁴ Na_2CO_3 ,^{15,16} NaHCO_3 /glycerine,¹⁷ or thin solutions of dilute formaldehyde solution,¹⁸ or flowing solutions of dilute H_2O_2 ¹⁹ have been used. For the final analytical measurement, ion chromatography, flame photometry, or flow-through absorbance/fluorescence detection has been used. For the tubular diffusion scrubbers, porous poly(tetrafluoroethylene)^{11,20} and porous polypropylene tubes¹² have been used. A new material, expanded PTFE, has been shown in allied experiments to exhibit very high transfer rates because of large internodal distances between fibrils and a thin wall.^{21,22} In these tubular membrane collectors, sample gas and absorbing solution flows are separated by the membrane and are generally countercurrent. Planar membrane collectors have been reported as well.^{23,24} We had developed a planar continuous flow scrubber in which the two conductivity electrodes were separated by the scrubber itself.²⁵

In the present device, microfabricated electrodes are integrated in the scrubber block, and the system is operated in the stopped-

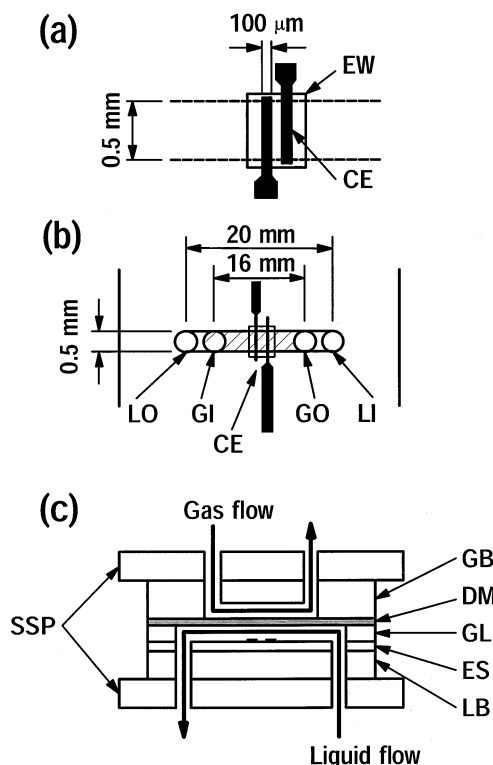


Figure 1. Structure of the scrubber/detector. (a) Close-up of the conductivity electrode; (b) top view of the arrangement. (c) Cross-sectional view: EW, electrode window; CE, platinum conductivity electrode; LI, liquid inlet; LO, liquid outlet; GI, gas inlet; GO, gas outlet; SSP, stainless steel plates; GB, gas flow block; DM, gas diffusion membrane; GL, gasket for liquid flow channel; ES, glass-epoxy substrate with conductivity electrodes; and LB, liquid flow block.

flow mode, eliminating the need for accurate liquid flow rate control. Sensitivity can be traded for time resolution. All presently available SO_2 analyzers, whether based on solution conductometry or UV fluorescence,²⁶ require a main power supply that is AC. The present device operates on low-voltage DC with a low power consumption, facilitating field deployment both in indoor and outdoor environment. Device performance was optimized through the detailed investigation of the membrane and absorber behavior. Details of performance, including comparative field data obtained in Mt. Aso, are presented.

EXPERIMENTAL SECTION

Gas-Absorbing Solution. The absorber was $5 \mu\text{M}$ H_2SO_4 containing 0.006% H_2O_2 and 10% 2-propanol (IPA). Reagent grade sulfuric acid and hydrogen peroxide (Wako Chemical) were mixed and diluted to 500 μM and 0.6% with deionized-distilled water, and the 100 \times stock absorber was stored refrigerated. The working solution was prepared by dilution of the stock followed by addition of IPA. The initial conductivity of the absorbing solution was 4.0 $\mu\text{S cm}^{-1}$.

Scrubber/Detector Construction. The structure of the hybrid gas collector detector is shown in Figure 1. A pair of

(7) *Continuous Analyzer for Sulfur Dioxide in Ambient Air*; JIS B 7952, Japanese Industrial Committee: Tokyo, 1977.

(8) Symanski, J. S.; Bruckenstein, S. *Anal. Chem.* **1986**, *58*, 1771–1777.

(9) Gáca, I.; Ferraroli, R. *Anal. Chim. Acta* **1992**, *269*, 177–185.

(10) Liu, S.; Dasgupta, P. K. *Anal. Chem.* **1995**, *67*, 2042–2049.

(11) Dasgupta, P. K.; Kar, S. *Anal. Chem.* **1995**, *67*, 3853–3860.

(12) Fish, B. R.; Durham, J. L. *Environ. Lett.* **1971**, *2*, 13–21.

(13) Durham, J. L.; Wilson, W. E.; Bailey, E. B. *Atmos. Environ.* **1978**, *12*, 883–886.

(14) Slanina, J.; Keuken, M. P.; Schoonebeek, C. A. M. *Anal. Chem.* **1987**, *59*, 2764–2766.

(15) Brauer, M.; Koutrakis, P.; Wolfson, J. M.; Spengler, J. D. *Atmos. Environ.* **1989**, *23*, 1981–1986.

(16) Brauer, M.; Koutrakis, P.; Spengler, J. D. *Environ. Sci. Technol.* **1989**, *23*, 1408–1412.

(17) Benner, C. L.; Eatough, D. J.; Eatough, N. L.; Bhardwaja, P. *Atmos. Environ.* **1991**, *25A*, 1537–1545.

(18) Keuken, M. P.; Schoonebeek, C. A. M.; Wensveen-Louter, A.; Slanina, J. *Atmos. Environ.* **1988**, *22*, 2541–2548.

(19) Simon, P. K.; Dasgupta, P. K. *Anal. Chem.* **1993**, *65*, 1134–1139.

(20) Komazaki, Y.; Hamada, Y.; Hashimoto, S.; Fujita, T.; Tanaka, S. *Analyst* **1999**, *124*, 1151–1157.

(21) Toda, K.; Dasgupta, P. K.; Li, J.; Tarver, G. A.; Zarus, G. M. *Anal. Chem.* **2001**, *73*, 5716–5724.

(22) Toda, K.; Dasgupta, P. K.; Li, J.; Tarver, G. A.; Zarus, G. M.; Ohira, S. *Anal. Sci.* **2001**, *17*, i407–i410.

(23) Guo, Z.; Li, Y.; Zheng, X.; Chang, W. B. ICAS 2001, Aug. 8, 2001, Tokyo, Japan; Abstracts, 2J08.

(24) Nagashima, K.; Fujihawa, Y.; Suzuki, S. *Anal. Chim. Acta* **1985**, *177*, 213–217.

(25) Toda, K.; Inoue, H.; Sanemasa, I. *Bunseki Kagaku* **1998**, *47*, 727–734.

(26) Schwarz, F. P.; Okabe, H. *Anal. Chem.* **1974**, *46*, 1024–1028.

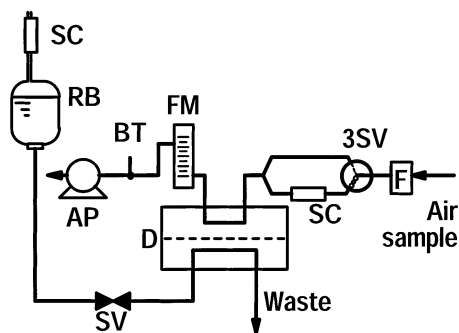


Figure 2. Fluid flow schemes: SC, soda-lime column; RB, reagent bottle containing absorbing solution; SV, solenoid valve; D, absorber/detector; F, filter; FM, flow meter; BT, ballast tube; and AP, air pump. The system is zeroed by powering on the three-way solenoid valve (3SV) to force gas flow through the SC.

platinum electrodes was first microfabricated on the glass-epoxy substrate ES as follows. The photoresist pattern was formed on ES by conventional photolithography with chlorobenzene treatment.^{27,28} Next, 60- and 200-nm-thick layers of Ti and Pt were respectively and successively deposited by radio frequency sputtering. Finally, the unwanted metal area was removed by lift-off. The width of each electrode and the separation between them were both 100 μm , as shown in the close-up view in Figure 1a. Enameled lead wires were connected to the bonding pads with an epoxy-based silver paste (EPO-TEK from Muromachi Kagaku Kogyo) and cured for 6 h at 130 $^{\circ}\text{C}$. The surface of the substrate and wires, except for the electrode window (EW), were coated with an oil-based paint layer. The gasket for liquid flow (GL), the gas diffusion membrane (DM), and the gas flow block (GB) were assembled in a stack on ES and held together between stainless steel plates (SSP) as shown in Figure 1c. This geometry results in the conductivity electrodes in the center of the absorbing area.

DM consisted of a membrane of porous Teflon (PTFE, pore 3.0 μm , thickness 75 μm , Advantec T300A25A, Toyo Roshi Ltd.) or porous polypropylene, (PP, pore 0.1 μm , thickness 89 μm , Gelman Metrical M5PU025, Pall Co.) membrane. The PP membrane had a glossy and a matte finish on opposite sides. Experience has shown that substantially better results are obtained with the glossy side of the membrane contacting the gas phase. A 100- μm -thick clear polyester sheet (used in overhead transparencies) or a 500- μm PTFE sheet was used as GL. A 0.5 \times 20-mm slit was formed in the sheet by an ultrasonic cutter. A small groove (0.5 mm in width, 1 mm in depth, and 16 mm in length) was formed on the plastic GB for the gas flow to correspond to the slit in GL, and GL was in fluid connection to the off-device liquid reservoir.

Measurement System and Procedure. The measurement system used is shown in Figure 2. A miniature air pump and a reagent bottle containing the absorbing solution were connected to the collector/detector. The reagent bottle was vented via a soda lime guard cartridge to prevent intrusion of SO_2 . The gas and liquid flow directions were countercurrent. The reagent bottle was placed at a hydrostatic height of 48 cm height relative to GL; this generated a liquid flow of 200 $\mu\text{L}/\text{min}$ when the normally closed solenoid valve (SV), placed just before the device, was opened.

To initially wet the membrane, 1 mL of IPA was injected into the solution channel of the device from the liquid inlet (LI) with air flowing on the other side. This process was repeated three times with 5-min intervals.

Measurement was made in the stopped-flow mode. With no power applied to the SV, there was no absorber liquid flow. As SO_2 dissolves in the solution and is oxidized irreversibly, the solution conductivity is increased. When the SV was powered open, the solution was pushed out by gravity and was exchanged by fresh absorber. The periodic opening and closing of the SV operation was conducted by the digital output from a small data logger (8420, Hioki Electric Co.), and the conductivity signal was stored in a CompactFlash card in the logger. The conductivity signal was obtained with homemade electronics assembled on a printed circuit board. A 1 kHz sine wave (2 V p-p), generated by a waveform generator chip (ICL8038, Harris), was applied to the electrode. The resulting alternating current was converted into DC voltage and amplified. The amplifier gain could be easily varied to obtain a wide dynamic range.

In a typical test procedure, the test gas was prepared by serial flow dilution of 1000 ppm SO_2 in N_2 standard (Sumitomo Seika), and a 0.20 SLPM (standard liter per minute) gas flow was sampled through the device with the help of a mass flow controller (SEC-410, STEC Inc.). In a series of experiments, we also investigated the effect of pressurizing the gas side of the device. In this case, the test gas flowed through the device as controlled by a mass flow controller, and an adjustable needle valve was added at the gas flow exit, the backpressure being monitored by a differential manometer (PS) (PA400-102G, Nidec Copal Electronics Co.). The whole system, including the data logger, was operated for extended periods from a small 12-V automotive battery.

RESULTS AND DISCUSSION

Flow Mode, Response Curve and the Choice of Membrane. If operated in the continuous flow mode, accurate liquid flow control is required, because the absorption time and, hence, sensitivity are inversely proportional to the flow rate. Therefore, a very stable pumping system is needed. Furthermore, the pump must be essentially noise-free, because a small collector/detector is particularly sensitive to flow noise. A pump that fits these requirements, such as a syringe pump, consumes too much power and represents a significant size and weight, as well. None of these facilitates a small portable field-deployable instrument. In contrast, the stopped-flow mode of operation adopted here eliminates these difficulties. The absorbing time is easily controlled by the choice of the SV periodicity. Placing the conductivity electrodes within the collector allowed real-time monitoring of conductivity increase during sampling.

Examples of response curves are shown in Figure 3. For the PP membrane, the conductivity increases continuously with a constant slope during sampling, and for both membranes, the conductivity returns rapidly to the original value as the SV is powered. Even without SO_2 , there is some gradual increase in conductivity due to evaporation. However, at least for the PP membrane, this is well below 5 ppbv SO_2 equivalent. Several PTFE membranes were initially examined. We made the puzzling observation that the conductivity becomes saturated relatively rapidly. This was not observed with the PP membranes, even though the rate of SO_2 transport through the PP membrane is

(27) Mimura, Y. *J. Vac. Sci. Technol.* **1985**, B3, 15–21.

(28) Fathimulla, A. *J. Vac. Sci. Technol.* **1985**, B3, 25–27.

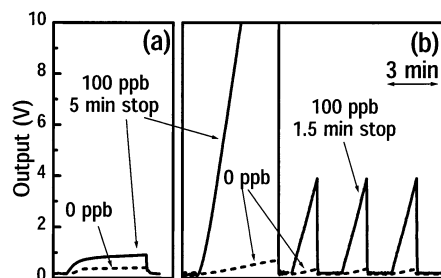


Figure 3. Typical response curves obtained with (a) PTFE and (b) PP membranes. The PTFE membrane was Advantec T300A025A, and the PP membrane was Metrice M5PU025. The gas phase was back-pressured at 0.78 and 7.8 kPa for the PTFE and the PP membranes, respectively, with a gas flow rate of 0.2 SLPM. The gasket was 100 μm in thickness.

obviously very much greater. Indeed, an absorption time of 1.5 min was found to be more appropriate for a 0–100 ppbv measurement range with this membrane. The water loss through the PTFE membrane was measured to be 7 times greater than that through the PP membrane. (A 300- μm -i.d. PTFE tube was connected to the device and set horizontally at the same height as the device. The water in the tube was aspirated to the device by evaporation, and the evaporation rate was computed from the rate of movement of the water–air interface in the tube.) We thus believe that for the PTFE membranes, such rapid evaporation results in a stagnant layer of relatively concentrated H_2SO_4 at the membrane interface that inhibits further uptake of SO_2 . In addition, the stagnant layer mixes rather slowly with the bulk solution. The loss of solution is made up by the influx of liquid from the open drain side of the device that effectively dilutes the region near the electrodes. As a result, after the initial rise, the rate of conductivity increase slows dramatically and attains a virtual plateau.

Obviously, the choice of the membrane is very important to realize good device performance. The performance of several membranes was tested and is listed in Table 1. The bubble point (superincumbent pressure at which air from the outside begins to go through the membrane pores and form a bubble in the internal liquid), the evaporation rate, and the gas transfer rate constant were experimentally determined. The gas transfer rate constant k was calculated from the initial slope of the conductivity increase using the following equations

$$\Delta C_{\text{SA}} = \frac{C_{\text{SA}}^0 (S - S_0)}{S_0} \quad (1)$$

$$k = \frac{V \Delta C_{\text{SA}}}{C_{\text{g}} A t} \quad (2)$$

where the initial H_2SO_4 concentration is C_{SA}^0 , and the increase in the H_2SO_4 concentration, ΔC_{SA} , is obtained from the relative increase of the conductivity signal, $(S - S_0)/S_0$. The gas transfer rate constant is the mass of H_2SO_4 collected ($V \Delta C_{\text{SA}}$, where V is the internal liquid collection volume) per unit time (t), membrane area (A), and gaseous SO_2 concentration C_{g} . The gas flow rate was held constant at 0.2 SLPM. Except in case of the PP membrane at sampling rates below 0.2 SLPM, the results would not have been influenced, because the amount of SO_2 actually

collected by the device is small relative to the sampling rate. We had previously tested²⁸ PTFE membranes from other vendors and found that the gas transfer rate constant was more acutely dependent on the membrane thickness than the pore size. In the present work, Advantec PTFE membranes were found to be better than the above for SO_2 collection. Between two types of Advantec membranes with the same thickness, the larger pore membrane showed greater SO_2 transport rate. Thus, the 3.0- μm -pore Advantec was the best PTFE membrane tested, and unless otherwise so stated, this membrane is referred to as the “PTFE” membrane. Although many initial experiments were conducted with the PTFE membrane, the PP membrane was found later to be much better. The SO_2 transfer rate constant was $>3\times$ better than the best PTFE membrane, and furthermore, the water evaporation rate was much lower.

Effect of Gas Flow Rate. Figure 4 shows a relationship between the gas flow rate and the device output signal for 100 ppbv SO_2 . The gas sampling time was 1.5 min for both the PTFE and PP membranes. In the case of the PP membrane, the response increased linearly with increasing sampling rate up to a flow rate of 0.2 SLPM and attained a virtual plateau thereafter. This is characteristic of a device in which collection is limited by diffusion through the membrane. For PTFE, only in the low flow range, a slight flow effect was observed with a sampling duration of 1.5 min. When the sampling duration was extended to 5 min, the final output was essentially independent of the sampling rate. On the basis of these results, a sampling rate of 0.2 SLPM was chosen for all further experiments.

Effect of Differential Transmembrane Pressure. Although membrane-based gas collectors have been used by a number of investigators,²⁹ to our knowledge, an effect of the differential pressure across the membrane has never been studied. Several different effects are a priori expected. First, in a Henry’s law-based system, solubility will increase with increasing absolute pressure. This may not be terribly relevant in the present case in which the uptake of SO_2 is ultimately due to reactive dissolution. Second, with increasing pressure on the membrane, the gas–liquid interface moves closer to the liquid side. This would increase the rate of uptake, since diffusion in gas phase is much faster than in the liquid. Third, whatever the initial moisture content of the sample may be, the difference in the water vapor pressure between the gas and liquid sides decreases with increasing absolute pressure; this should decrease evaporation. Obviously, the limit of increasing pressure on the gas side is controlled by (a) the bubble point of the membrane and (b) the ability to pressurize the sample gas in any real sampling situation (this necessitates a suitably inert pump, such as a fluorocarbon diaphragm pump). We attached a needle valve downstream of the collector/detector, and the transmembrane pressure was controlled by adjusting this valve while a constant air flow was maintained. Although the range of transmembrane pressure attainable in this manner was limited by the bubble point and was rather small (<1 to several kPa), the effect of transmembrane pressure was readily discernible. As can be seen from Figure 5, the blank decreased and response increased with the backpressure. Especially for the PTFE scrubber, the original signal/blank ratio is small, and the improvement

(29) Dasgupta, P. K. in *Sampling and Sample Preparation Techniques for Field and Laboratory*; Pawliszyn, J. Ed.; Elsevier: New York, in press.

Table 1. Comparison of the Gas Diffusion Membranes

manufacturer	product	material	pore size μm	thickness μm	bubble point kPa	evaporation $\mu\text{L}/(\text{min cm}^2)$	transfer rate constant ^a $\text{fmol}/(\text{s cm}^2 \text{ ppbv})$
Flonchemical	Floropore NP-022	PTFE	0.22	60	3.9		10
Flonchemical	Floropore NP-100	PTFE	1.0	100			7.5
Flonchemical	Floropore NP-200	PTFE	2.0	100			8.4
Millipore	LCWP025	PTFE	10	125			5.6
Toyo Roshi	Advantec T080A025A	PTFE	0.8	75	2.4		19
Toyo Roshi	Advantec T300A025A	PTFE	3.0	75	0.98	13.6	32
Pall	Gelman Metrcel M5PU025	PP	0.1	89	9.8	1.99	105

^a The SO_2 permeabilities were calculated from the initial increasing rate of the conductivity.

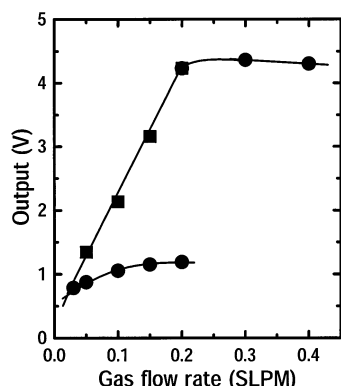


Figure 4. Effect of the gas flow rate. The symbols ● and ■ are responses to 100 ppbv SO_2 with PTFE and PP membranes, respectively. Backpressures of 0.78 and 7.8 kPa were applied to the PTFE and PP membranes, respectively. In both cases, the thickness of the gasket was 100 μm , and the gas sampling time was 1.5 min.

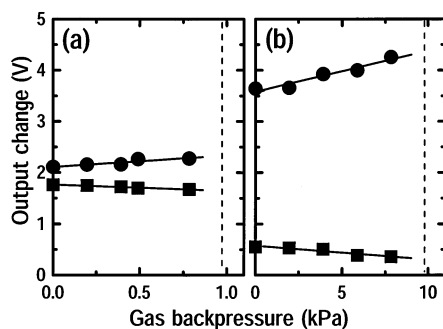


Figure 5. Effect of differential pressure across membrane. Panels a and b were obtained with the PTFE and PP scrubbers, and ■ and ● indicate output data of blank and 100 ppbv SO_2 . The dashed lines represent the bubble point of the respective membranes. The gas flow rate was 0.2 SLPM; other conditions were same as those in Figure 4.

in the signal-to-blank ratio with the transmembrane pressure was significant. Although we have not as yet implemented the backpressurization technique for actual measurements, these results do establish that such a method can be attractive, at least for cases in which a suitably inert pump is available.

Effect of Liquid Layer Thickness. The amount of the analyte gas collected, Q , was proportional to the gas transfer rate constant, k ; the effective membrane area, A ; the analyte gas concentration, C_g ; and the absorbing time, t .

$$Q = kAC_g t \quad (3)$$

The increase in the H_2SO_4 concentration, ΔC_{SA} , is obtained by

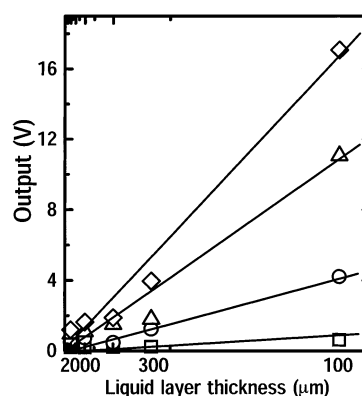


Figure 6. Effect of liquid layer thickness. PP membrane, gas flow rate 0.2 SLPM, transmembrane pressure 7.8 kPa, sampling time 1.5 min. □, ○, △, and ◇: 0, 100, 300 and 500 ppbv SO_2 , respectively. The abscissa is the liquid layer thickness with a reciprocal scale.

dividing Q by the absorber solution volume V . Thus, ΔC_{SA} is inversely proportional to A/V , namely, to the solution thickness, δ .

$$\Delta C_{\text{SA}} = \frac{Q}{V} = \frac{kAC_g t}{V} = \frac{kC_g t}{\delta} \quad (4)$$

Equation 4 predicts that the thinner the solution layer, the greater would be ΔC_{SA} and, thus, the conductivity and detection sensitivity. This was experimentally confirmed. For collectors of planar design, the solution thickness, δ , could be easily changed by replacement of the spacer. The thickness, δ , was varied between 100 and 2000 μm , and the results are shown in Figure 6, which plots the liquid layer thickness in reciprocal scale as the abscissa vs the conductivity output as the ordinate for 0, 100, 300, and 500 ppbv SO_2 test samples. (It should be noted that all blank experiments involved completely dry air; the blank signal that is thus observed due to evaporation is the maximum value of the blank.) The results show conformity to eq 4, and the lowest thickness tested in this series (100 μm) provided the best sensitivity. However, further reduction in δ with 25- and 50- μm polyimide (Kapton) spacers did not produce consistently good results. In these cases, the membrane was flexible enough to irreproducibly contact the electrodes, and results were inconsistent. Accordingly, further work was performed with a δ value of 100 μm . The computed effective solution volume, V , is 800 nL, to our knowledge, the lowest reported of any liquid-based gas collector.

Calibration Behavior. Figure 7 shows calibration curves obtained under the optimized conditions. As shown in the left

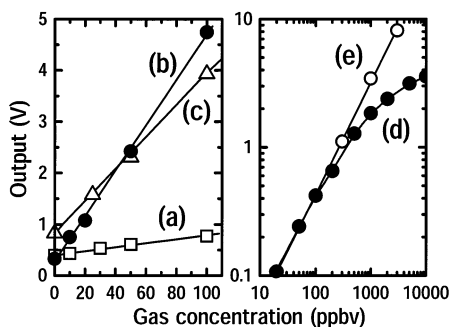


Figure 7. Calibration behavior. Left: 0–100 ppbv response for (a) PTFE, 0.78 kPa backpressure; (b) PP, 7.8 kPa backpressure; (c) PP, no backpressure. Right: response of PP, 7.8 kPa backpressure, over a wide range of SO_2 concentrations, shown in a log–log plot. (d) 0.006% H_2O_2 same as curves a–c; curve e 0.6% H_2O_2 .

panel of Figure 7, linear curves with good correlation were obtained from 0 to 100 ppbv for both (a) the PTFE and (b, c) the PP collectors. Curve c was obtained without any backpressure. The detection limits (LODs) obtained for the PP were 0.7 and 1.0 ppbv for the experimented conditions used to generate curves b and c, respectively. The LODs were determined from the slope of calibration curves and three times the standard deviation of the blank values obtained at 25 °C with dry air. Although we have not explicitly tested this, the measurement principle is such that the sampling period can be extended to further reduce the LOD, or time resolution can be further improved if only higher concentrations are measured. The right panel in Figure 7 shows the results over a much wider measurement range in a log–log format (obtained at $10\times$ lower gain than the left panel). With an H_2O_2 content of 0.006% as used in the other experiments, the calibration deviated from linear behavior at high SO_2 concentrations, as in curve d. With an increase in H_2O_2 content of 0.6%, good linearity was observed up to 3 ppmv SO_2 , as in curve e.

It is interesting to note that the small dimensions of the collector and the stopped-flow mode of operation sets the upper limit of applicability. We were initially surprised that when several-parts-per-million-volume SO_2 was tested with the 0.6% H_2O_2 absorber, bubbles were invariably generated in the device, making measurements impossible. Further reflection indicated that the collector solution volume is so small that the heat generated due to the reactive dissolution of 10 ppmv sampled SO_2 will result in a temperature rise of 40 °C under adiabatic conditions!

Effect of IPA on System Hysteresis and Reproducibility.

The response behaviors of the system over a several hour period of time accompanied by step changes of gaseous SO_2 concentration are shown in Figure 8. The only difference in the top and bottom panels is the inclusion of 10% IPA in the absorber in the latter. It is obvious that there is a very perceptible decrease in rise and fall times, as when IPA is present. What is less obvious is that the reproducibility of response to defined concentration steps was significantly poorer without IPA. In the absence of IPA, the memory effect was particularly easily observed when the step change in the SO_2 concentration was large. The results indicate membrane surface wetting and sweeping of dissolved/absorbed SO_2 from this region was vastly improved with the presence of IPA. Without the initial IPA wash of the membrane as described in the Experimental Section, the initial response was very small. Further, it took a very long time to attain a stable high sensitivity.

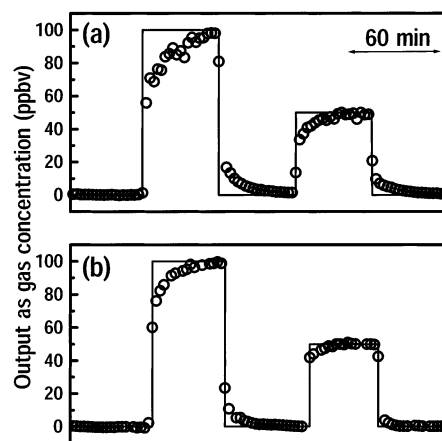


Figure 8. Effect of IPA on response behavior. The solid lines indicate the temporal variations in the SO_2 concentrations sampled by the test system, and the circles indicate device response. Panels a and b indicate behavior without and with 10% IPA in the absorber, respectively.

Table 2. Interference Test

test gas	test concn ppmv	abs interference equiv ppbv SO_2	rel interference %
NO	5.0	18	0.36
NO_2	5.0	170	3.5
H_2S	5.0	20	0.40
CO_2	5000	17	0.000034
NH_3	0.050	−4.7	−9.3
	1.0	15	1.5

Without IPA in the absorber, this initial IPA conditioning was needed every time the device was used each day. With IPA in the absorber, once operation was started with a new device, this treatment was needed only when the membrane was replaced.

Interference of Other Gases. For conductometric measurement with a membrane-based collector, it may seem that any gas that diffuses through the membrane and interacts with the reagent in the absorbing solution can interfere. In reality, for significant interference to occur, the gas must (a) exhibit good equilibrium solubility (high Henry's law constant) under acidic conditions and (b) either in dissolved form or after reaction with H_2O_2 , significantly change the proton concentration of the absorber, the proton being by far the biggest contributor of conductivity of the absorber. Interference of this device as examined with NO, NO_2 , H_2S , CO_2 , and NH_3 are presented in Table 2. It would be readily apparent that at realistic concentrations, none of the acid gases would interfere in any practical manner unless the atmospheric concentrations are highly unusual. It should be noted that of all the common acid gases tested above, SO_2 not only is by far the most strongly acidic gas, it has the highest intrinsic Henry's law solubility. Moreover, as SO_2 dissolves and is oxidized and the liquid becomes consequently more acidic, the rate of the oxidation of the dissolved S(IV) actually increases with decreasing pH.^{30,31}

In contrast to the acid gases, the interference of NH_3 was not only significant, as may be expected, it was also in the opposite direction, because uptake of ammonia results in the conversion

(30) Martin L. R.; Damschen D. E. *Atmos. Environ.* **1981**, *15*, 1615–1621

(31) McArdle J. V.; Hoffmann M. R. *J. Phys. Chem.* **1983**, *87*, 5425–5429.

of the protons present to less conductive NH_4^+ . However, ammonia is a basic gas with high diffusivity and is easily removed by a relatively short length of an acid-coated diffusion denuder. At the inlet, a 15-cm length of a tube coated with KHSO_4 or citric acid¹⁸ completely removed any effect of 10 ppbv NH_3 . This would be among the highest levels of ambient ammonia encountered under most circumstances. It should also be noted that in real atmospheres, the concurrent existence of high levels of both NH_3 and SO_2 is very unlikely as a result of oxidative conversion to ammonium sulfate aerosol.

Field Application. The SO_2 measurement system was field-tested at Kusanenri in Mt. Aso over several days. The data are shown in comparison with results obtained with a conventional solution-conductivity-based commercial SO_2 measurement instrument (model SX-07, Kyoto Denshi Co.). As a matter of comparison, this instrument was 1.2 m in height and equipped with two 20-L solution reservoirs. The measurement involved direct bubbling of the sample gas through an impinger containing 20 mL of absorbing solution. The field location in Kusanenri (latitude $32^\circ 53'$, longitude $131^\circ 3'$, and altitude 1150 m), was in green highlands 3 km west of a fumarole. The typical background concentration measured (~ 2 ppbv) was actually lower than concentrations we typically measure in our home laboratory in Kumamoto City, 30 km west of Mt. Aso. However, there are occasional spurts of SO_2 concentration when fumarole emissions and wind direction coincide, as shown in Figure 9 for April 11, 2002. Hydrogen sulfide concentrations were simultaneously measured with a collocated fluorometric instrument.^{24,25} The results clearly indicate that the increases in SO_2 and H_2S concentration are strongly correlated and, thus, likely have the same volcanic origin. Comparison with the data generated by the conventional instrument indicates general agreement, but temporal resolution and accurate measurement of rapidly changing concentrations are obviously very much better with the present device. Thus, the device showed good time resolution comparable to an UV-fluorescence instrument that is large, expensive, and needs an AC power source. At low levels of SO_2 , the commercial instrument also tends to show higher levels. It has been reported that the conventional conductivity-based instruments do tend to produce higher results.³² We checked interference of the JIS bubbler method⁷ from relatively high levels

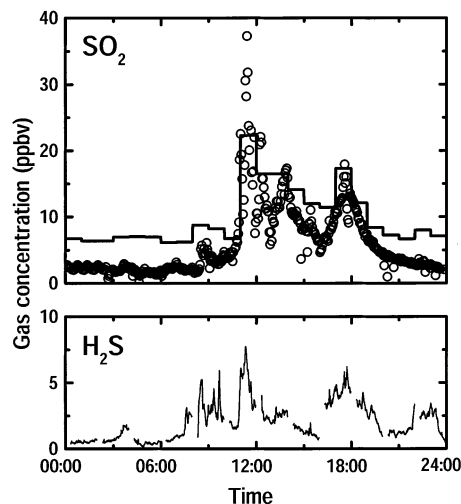


Figure 9. Field test data obtained at Kusanenri in Mt. Aso on April 11, 2002. Circles indicate 3-min-resolution SO_2 data obtained by the instrument. The solid line represents SO_2 data obtained with conventional conductivity instrument with 1-h resolution. Lower panel shows concurrently measured H_2S concentration.

(100 ppbv) of NO_2 ; no interference was observed. The reason that this method tends to produce higher readings compared to our instrument at low levels of SO_2 is likely because ionic aerosol constituents that are scrubbed by the impinger raise the conductivity in the commercial instrument. In contrast, it is known that membrane-based collectors do not suffer from interference from aerosols.^{23,32}

CONCLUSIONS

In summary, we have described a miniature hybrid practical device that is sufficiently sensitive for the measurement of ambient levels of SO_2 with sufficiently rapid response. Such devices are mass-manufacturable at relatively low cost. A number of developments have taken place in recent years toward sensitive but affordable fluorescence and absorbance measurements with solid-state sources and detectors, and the general approach that we describe here should be applicable to a number of other gases and other chemistries.

Received for review July 15, 2002. Accepted September 17, 2002.

AC025940B

(32) Sakai, K.; Sakata, M.; Takata, Y. *Kankyo Bunseki notameno Kikibunseki*; Nippon Kankyo Sokutei Bunseki Kyokai: Tokyo, 1995; p 435.